CONF-8810231--8

Pellet Ablation and Temperature Profile Measurements in TFTR*

D. K. Owens, G. L. Schmidt, A. Cavallo, B. Grek, R. Hulse,
D. Johnson, D. Mansfield, D. McNeill, H. Park, and G. Taylor

Princeton University, Plasma Physics Laboratory
Princeton, NJ 08543 USA

and

W. A. Houlberg, S. L. Milora, and S. E. Attenberger

Oak Ridge National Laboratory
Oak Ridge, TN 37831 USA

CONF-8810231--8

DE89 008924

AC-5-84-12140

1. INTRODUCTION

Single and multiple deuterium pellets have been injected into a variety of TFTR plasmas, including ohmically heated plasmas with a wide range of electron temperatures, neutral beam heated plasmas at several NBI powers and high T_e, post NBI plasmas. Pellet penetration into these plasmas was determined by measuring the pellet speed and duration of the H_α/D_α light emission during pellet ablation in the plasma. These penetration measurements are compared to the predicted penetration computed using the ablation model developed by Oak Ridge National Laboratory [1]. The plasma density profiles before and after pellet injection are used to estimate the number of particles deposited in the plasma. The plasma particle increase compared to the estimated number of atoms in the pellet yields a measure of the fueling efficiency of pellets in TFTR. The ablation cloud parameters are discussed based on polychromater measurements of the H_α/D_α line emission from the neutral cloud surrounding the pellet. The electron temperature profile evolution after pellet injection is examined for the case of multiple pellet injection into an ohmically heated plasma.

These experiments were carried out using the Deuterium Pellet Injector (DPI) developed and fabricated by the Oak Ridge National Laboratory. The DPI has eight single shot barrels. There are three 3 mm diameter, three 3.5 mm, and two 4.0 mm diameter barrels which fire cylindrical pellets 3.4 mm long at speeds of up to 1.5 km/s for deuterium pellets. The 4.0 mm diameter pellets contain approximately 3×10^{21} particles resulting in a typical increase in plasma particles of $\Delta N/N \approx 3$.

The ORNL pellet ablation code was used to compare measured pellet penetration depths with a theoretical model. The measured input parameters to the model are the electron density and temperature profiles, the neutral beam heating profile, the neutral density profile, the pellet size, pellet speed and pellet composition. The free parameter in the model is the thickness of the neutral cloud surrounding the pellet. This parameter is adjusted to arrive at a reasonable agreement between measured and calculated pellet penetration depths. The output of the model which is directly comparable to experiment is the calculated ablation rate. It is assumed that the broad-band H_α/D_α emission is proportional to the ablation rate. It is certainly true that the termination of the broad-band emission marks the maximum penetration depth of the pellet.

2. PELLET PENETRATION STUDIES

The penetration of deuterium pellets into TFTR plasmas is determined from the termination time of the D_α emission from the ablating pellet. This time combined with the measured pellet speed, firing time, and machine geometry yields the absolute penetration depth of the pellet into the plasma. Three cases have been investigated so far: 3.0 and 3.5 mm pellets into ohmically

*Research supported by U.S. Department of Energy contract No. DE-AC02-76-CHO-3073.

DISTRIBUTION OF THIS DOCUMENT IS UNLIMITED

heated plasmas and 4.0 mm pellets into neutral beam heated plasmas. In each case, the penetration depth was calculated with the ORNL ablation model using profiles which were either measured or calculated with the SNAP [2] one-dimensional, time independent analysis code.

The results of this survey are shown in Fig. 1 for the three cases. The neutral cloud thickness was adjusted to 0.5 mm to give reasonable agreement between measured and calculated penetration depths for the 3.0 mm pellets into ohmically heated plasmas. This value was then used for all subsequent penetration calculations. The 3.0 mm pellets were chosen as the base line case for determining the neutral cloud thickness as this situation best represented the assumptions in the ORNL model used. These pellets did not penetrate deeply into the plasma and hence did not cross any low-q rational flux surfaces. An example of this shallow penetration ohmic case is shown in Fig. 2. The measured broad-band D_α emission is plotted along with the calculated ablation rate in arbitrary units. The termination point of both curves is in good agreement though the detailed agreement between the two curves is perhaps poorer. The discrepancy between the measured and calculated ablation in the outer region of the plasma is typical.

The 3.5 mm pellets penetrated much deeper into the ohmically heated plasmas in TFTR because larger pellets penetrate deeper and with the DPI, larger pellets tend to be faster. It can be seen from Fig. 1 that the agreement between calculated and measured penetration for the 3.5 mm pellets is poor. A typical example of calculated and measured ablation is shown in Fig. 3 for these larger pellets. In contrast to the 3.0 mm pellets, there is considerable structure in the emission from the 3.5 mm pellets. Sawteeth were present in both cases during pellet injection. There is a strong decrease in emission at the plasma center and at a radius near the q=1 surface. The ORNL ablation code does not model rational q surfaces though the limited volume of the plasma center is taken into account. For these deep penetration cases where the pellet ablation decreases at rational q surfaces, good agreement between theory and experiment is not to be expected. However, the model does predict that the pellet will penetrate well into the plasma, insuring central fueling. Note that there is still a discrepancy in the outer plasma between the modelled and measured ablation rate.

The agreement between measured and calculated penetration depths for the NBI cases is also poor. The model reproduces the general features of the observed D_α emission such as increased emission in the outer plasma region but overestimates the observed ablation rate. However, high energy ion ablation is important both in the model and in the experiments. Simulating the ablation without including the high energy ion ablation leads to much too deep pellet penetration. That high energy ion ablation is experimentally important is seen in Fig. 4. Shown in Fig. 4(a) is the broad-band emission from a 3.5 mm pellet injected at 2.4 s into an ohmically heated plasma with $T_e(0) = 3.2$ keV. Sawteeth are present in the plasma at this time. The pellet penetrates well past the center of the plasma. In Fig. 4(b) is the emission from a 4.0 mm pellet injected at 3.0 s into the same discharge as in Fig. 4(a), but with 5 MW of neutral beam heating and $T_e(0) = 2.0$ keV. Sawteeth are no longer present, having been supressed by the first pellet. Both pellets had a speed of 1.48 km/s. If high energy ion ablation were not important, the second pellet, being larger and in a lower temperature plasma, would have penetrated much deeper than the first pellet and would probably not have been completely ablated in the plasma.

3. PELLET FUELING STUDIES

For a number of the cases shown in Fig. 1, it was possible to determine the particle content of the plasma before and after pellet injection. The fueling efficiency, defined as the increase in the particle content of the plasma divided by the number of particles in an ideal pellet, is shown in Fig. 5 for these cases plotted against measured penetration depth. It should be noted that photographs of pellets do not show the pellets to have an ideal cylindrical shape but rather to be somewhat rounded at the ends. The definition of fueling efficiency used here will overestimate the number of particles in the pellet and hence systematically underestimate the fueling efficiency.

It can be seen from Fig. 5 that there is an increase in fueling efficiency with penetration depth for the 3.5 mm pellets injected into ohmically heated plasmas. This effect is real and not a result of variability of nominal pellet size. If a pellet were larger than expected it would penetrate farther into the plasma and appear to fuel more efficiently, having more particles than the average pellet. In fact, the differences in pellet penetration depth are due to differences in target electron temperature and pellet speed. Pending a better assessment of the actual number of particles in a pellet, the absolute fueling efficiency cannot be determined but it is at least 50% increasing to 75% with penetration depth.

The fueling efficiency for the 4.0 mm pellets injected into neutral beam heated plasmas appears to be worse than for the ohmic case. The beam power was approximately 10 MW for the pellets which penetrated to 0.65 m and 5 MW for the pellet which penetrated to 0.8 m. The 5 MW case is the same as shown in Fig. 4. Due to the limited amount of data, it is not possible to discern any systematic trend in the NBI fueling efficiency data other than that the efficiency is less than for ohmic heating only.

A clear example of the lower fueling efficiency in NBI heated plasmas is shown in Fig. 6 which is a plot of the increase in plasma density from pellet fueling plotted *vs* major radius. In this example a 3 mm pellet was injected into an ohmically heated and an NBI (P_{NB} = 10 MW) heated plasma having approximately the same electron temperature and density. The smaller plasma density increase in the NBI case is not due to reduced pellet mass as then the pellet would not penetrate as deeply as it did. At present, there is no satisfactory explanation for the reduced fueling efficiency in NBI heated plasmas.

4. SPECTROSCOPIC MEASUREMENTS OF PELLET ABLATION

An eight channel polychromater has been used on TFTR to observe the D_α line emission from the luminous cloud surrounding the ablating pellet. The polychromater spans the spectral range from 630 nm to 665 nm. The measured spectra were analyzed to determine the electron density in the cloud from the Stark broadening of the D_α line and the electron temperature from the line-to-continuum ratio. Typically, $T_e = 1.6 \pm 0.3$ eV in the luminous cloud throughout the ablation process.

The observed spectrum has structure which yields information on the properties of the cloud. Channels near the line center have lower than expected intensity which is explained by self-absorption in the luminous cloud. Analysis indicates that the luminous cloud is a few millimeters thick.

Figure 7 shows the electron density and radiated power from the D_α line during the ablation of a pellet in TFTR. Figure 8 is a comparison of the broad-band emission from a three pellet sequence with the integrated D_α emission normalized at the peak intensity. There is good agreement between the line and broad-band emission, lending support to the use of broad-band emission as a measure of D_α line emission. To the extent that D_α line emission is proportional to the ablation rate, so is broad-band pellet emission.

5. T_e PROFILE EVOLUTION

A series of pellets were injected into an ohmically heated, I_p = 2.2 MA, q_{cyl} = 3 discharge [3]. The last pellet in the series fueled the center of the plasma and supressed sawteeth. Between 0.5 – 0.7 s after the last pellet, an intense central radiation loss develops due to brehmsstrahlung from the dense central plasma. During this time, the central radiation power density becomes a significant fraction of the ohmic input power while the electron temperature profile becomes hollow.

The density profile for $r/a \geq 0.4$, evolves from a peaked profile just after injection to a profile which is broader than the profile just before injection of the last pellet: $n_e(0.4)/n_e(0.8) = 1.72$ before injection and $n_e(0.4)/n_e(0.8) = 1.54$ at 0.7 s after injection, 10% broader. Figure 9 shows the time evolution of the density profile normalized to the density at $r/a = 0.5$. The curve at 2.6 s is the target density for the last pellet in the series which was injected at 2.74 s. The profile evolves significantly during the entire period shown.

After injection of the last pellet, the electron temperature for r/a $\geq$ 0.4 initially broadens from $T_e(0.4)/T_e(0.8)$ = 3.07 at 2.6 s just before pellet injection to $T_e(0.4)/T_e(0.8)$ = 2.65 at 2.9 s, 160 ms after pellet injection, a broadening of 15%. The profile shape rapidly evolves back to its pre-injection value so that 350 ms after pellet injection $T_e(0.4)/T_e(0.8)$ is within 5% of the pre-injection value. Figure 10 shows the electron temperature profile evolution. For r/a $\geq$ 0.4, there is little evolution of the profile shape even though the density and radiation profiles are still evolving significantly.

6. CONCLUSIONS

Measured pellet penetration into ohmically and NBI heated plasmas in TFTR have been compared to calculations using the ORNL pellet ablation code. In shallow pellet penetration in ohmic plasmas, the calculated pellet lifetime is in reasonable agreement with observations, though the calculated ablation appears too large in the outer region of the plasma. In deep pellet penetration in ohmic plasmas with sawteeth present, the calculated pellet lifetime is too short. A strong decrease in observed pellet ablation at the q=1 surface is not modelled. For pellet penetration into NBI heated plasmas where sawteeth were supressed by a previous pellet, the calculated pellet lifetime is too short. High energy ion ablation is important though, both experimentally and computationally.

Pellet fueling efficiency increases with increasing pellet penetration for deep penetration in ohmically heated plasmas, reaching values of 75% or more. The data for pellet fueling in NBI heated plasmas is not conclusive, but the fueling efficiency appears to be less than for the ohmic case.

The electron temperature profile evolves to its pre-pellet shape on a ~300 ms time scale. The shape of the outer half of the profile is largely unchanged by pellet injection even though the density and radiation profiles are still evolving and the central T_e profile is hollow.

REFERENCES

[1] Houlberg, W. A., Milora, S. L., Attenberger, S. E., Nucl. Fusion **28** (1988) 595.
[2] Towner, H. H., Goldston, R. J., Bull. Amer. Phys. Soc. **29** (1984) 1305.
[3] Taylor, G, Fredrickson, E. D., et. al., Nucl. Fusion **29** (1989) in press.

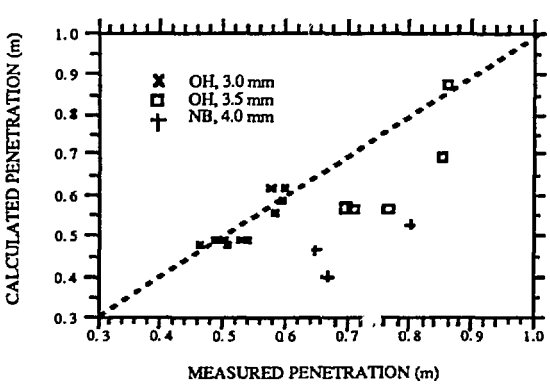

Figure 1: Calculated pellet penetration from the ORNL pellet code plotted against the measured penetration for 3.0, 3.5, and 4.0 mm diameter pellets. The neutral cloud thickness was 0.5 mm to match the 3.0 mm pellet data.

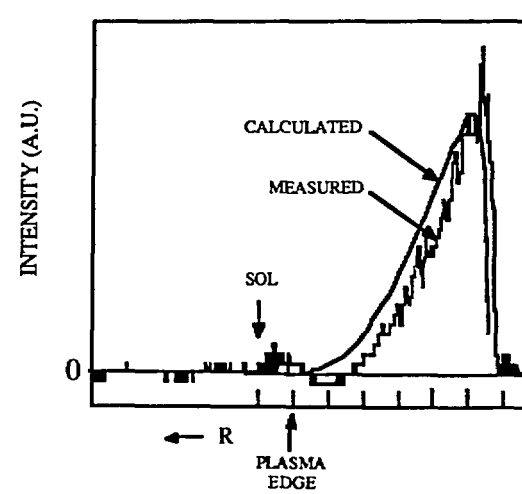

Figure 2: Comparision of measured broad-band emission and calculated ablation rate for a 3.0 mm pellet. Radius units are 10 cm.

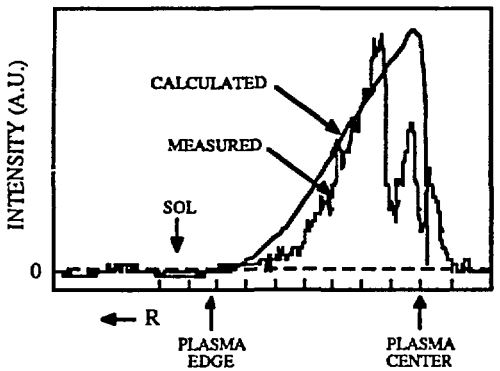

Figure 3: (above) Comparision of measured broad-band emission and calculated ablation rate for a 3.5 mm pellet. Radius units are 0.1 m.

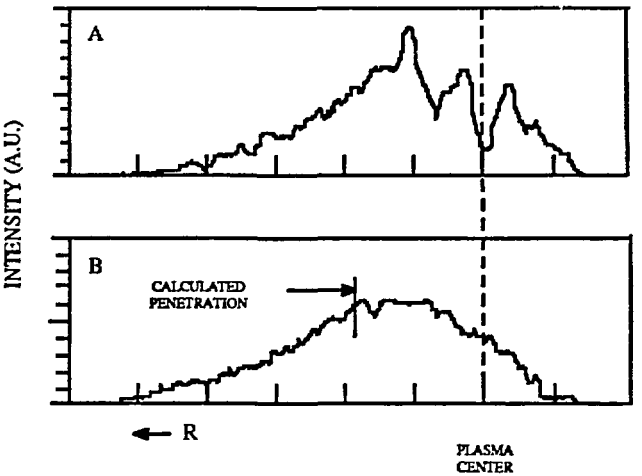

Figure 4A: (above) Broad band emission from a 3.5 mm pellet injected into the ohmic portion of shot 29615. The central electron temperature was 3.2 keV

Figure 4B: (above) Broad-band emission from a 4.0 mm pellet injected into the NBI portion of shot 29615. NB power was 5 MW and the central electron temperature 2.0 keV

Pellet speed: 1.48 km/s Plasma radius: 0.8 m
Radius units: 0.1 m

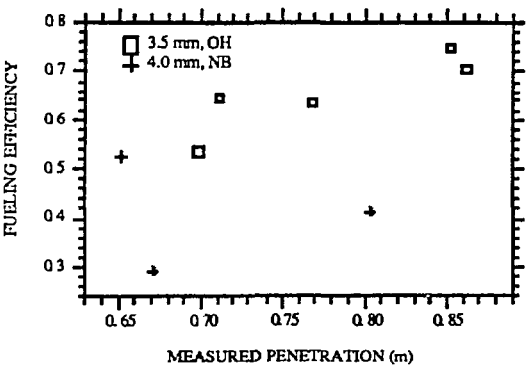

Figure 5: (above) The fueling efficiency of 3.5 mm pellets into ohmically heated plasmas and 4.0 mm pellets into NBI heated plasmas.

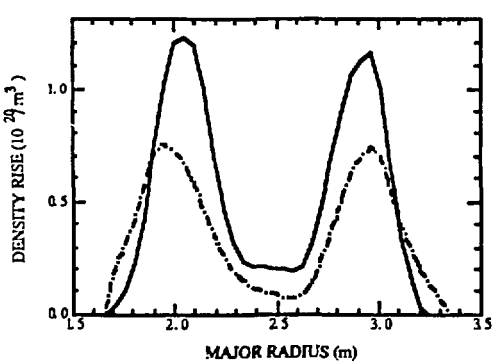

Figure 6: (left) The density rise from pellet fueling in an ohmically heated (solid) and NBI heated plasma (dashed). In both cases the pellets were 3.0 mm, the pellet speed was 1.05 km/s, the electron temperature was about 3.2 keV, and the plasma radius = 0.8m.

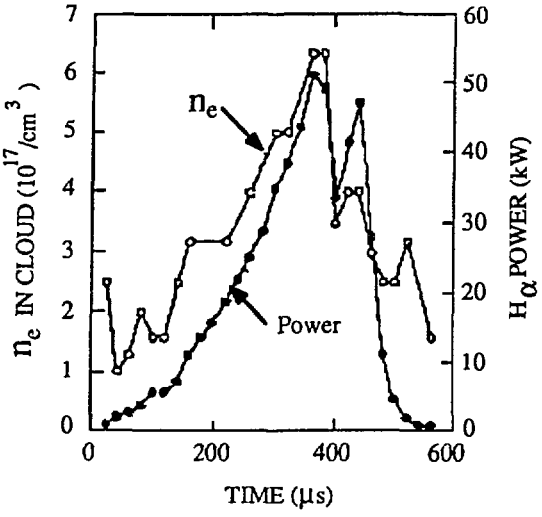

Figure 7: Electron density and radiated power from the luminous cloud surrounding an ablating pellet.

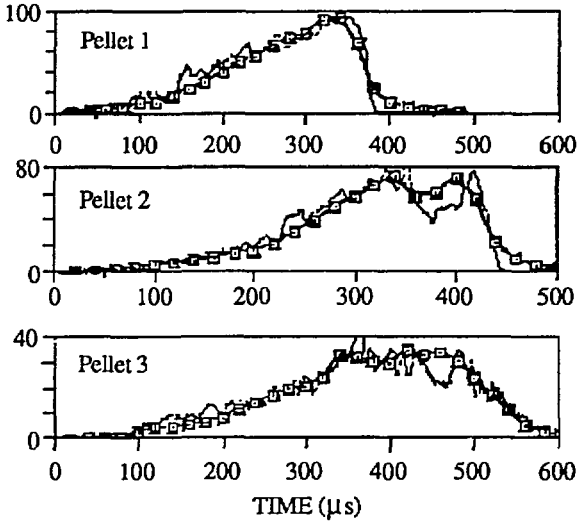

Figure 8: The power radiated in the D_α line compared to the broad-band radiation.
Squares – line radiation
Solid – broad-band radiation

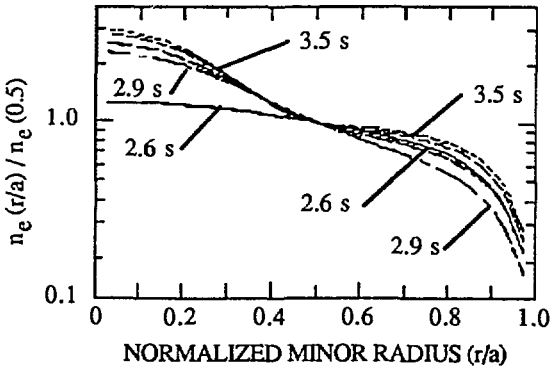

Figure 9: Evolution of the normalized density profile from a pellet injected at 2.74 s. The pellet penetrates to the plasma center.

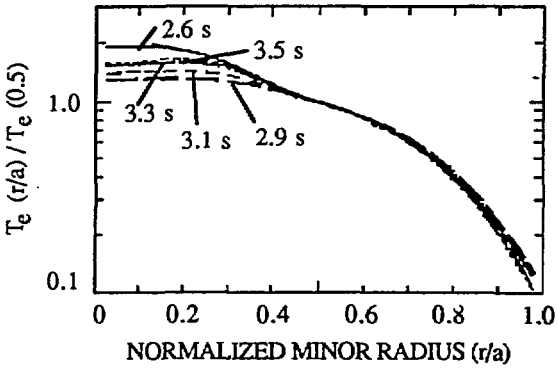

Figure 10: Normalized electron temperarure profile for the same situation as in Figure 9.

DISCLAIMER

This report was prepared as an account of work sponsored by an agency of the United States Government. Neither the United States Government nor any agency thereof, nor any of their employees, makes any warranty, express or implied, or assumes any legal liability or responsibility for the accuracy, completeness, or usefulness of any information, apparatus, product, or process disclosed, or represents that its use would not infringe privately owned rights. Reference herein to any specific commercial product, process, or service by trade name, trademark, manufacturer, or otherwise does not necessarily constitute or imply its endorsement, recommendation, or favoring by the United States Government or any agency thereof. The views and opinions of authors expressed herein do not necessarily state or reflect those of the United States Government or any agency thereof.